

## Numerical conformal mapping of multiply connected regions by Fornberg-like methods

Thomas K. DeLillo<sup>1</sup>, Mark A. Horn<sup>2</sup>, John A. Pfaltzgraff<sup>3</sup>

<sup>1</sup> Department of Mathematics and Statistics, Wichita State University, Wichita, KS 67260–0033, USA; e-mail: delillo@twsuvm.uc.twsu.edu

<sup>2</sup> ARINC, Inc., 6703 Odyssey Drive, Suite 104, Huntsville, AL 35806, USA; e-mail: mhorn@arinc.com

<sup>3</sup> Department of Mathematics, University of North Carolina at Chapel Hill, Phillips Hall, CB 3250, Chapel Hill, NC 27599-3250, USA; e-mail: jap@math.unc.edu

Received March 12, 1998 / Revised version received December 16, 1998

*Dedicated to Olof B. Widlund on the occasion of his 60th birthday*

**Summary.** We develop a new algorithm for computing conformal maps from regions exterior to non-overlapping disks to unbounded multiply connected regions exterior to non-overlapping, smoothly bounded Jordan regions. The method is an extension of Fornberg's original Newton-like method for mapping of the disk to simply connected regions. A Fortran program based on the algorithm has been developed and tested for the 2 and 3 disk case. Numerical examples are reported.

*Mathematics Subject Classification (1991):* 30C30, 65E05

### 1. Introduction

Many effective numerical algorithms are available for approximating conformal maps of simply and doubly connected regions where the unit disk and the annulus provide useful computational domains. In the multiply connected case, parallel, radial, and circular slit domains provide useful canonical domains, and there are analytic relations between various pairs of the corresponding mapping functions; see [Ne, Chapt. 7]. The circular domain [Go, He], that is, a domain that is the complement of a finite number of non-overlapping disks is the canonical domain we use as the computational

---

*Correspondence to:* T.K. DeLillo

domain in our present work. The circular domain is physically, geometrically, and computationally natural for many situations. In particular, the circular boundary components facilitate the use of Fourier methods. Most numerical conformal mapping methods for simply connected domains involve solving an integral equation for the boundary correspondence between the computational and the target domains, after some normalization of the map to insure uniqueness. In the multiply connected case, the conformal moduli must be computed along with the boundary correspondences.

In this paper, we develop a method for mapping a circular domain onto a region in the extended complex plane containing the point at infinity and bounded by a finite number of smooth Jordan curves. We will refer to this map as the *circle map*. Our work is inspired by the simply connected method in [Fo], and like that work, ours is a quadratically convergent Newton-like method for computing the boundary correspondences and, additionally, the centers and radii of the disks (the conformal moduli).

In his method for the disk, Fornberg [Fo] used the fact that a function defined on the boundary of the unit disk can be extended analytically to the interior if and only if the negatively indexed Fourier coefficients of the function are zero. We refer to these conditions for analytic extension as *analyticity conditions*. By linearizing about the current guess for the boundary correspondence, Fornberg used these analyticity conditions to develop an inner linear system for the Newton update of the boundary correspondence. He noted that this inner system was positive semi-definite with the eigenvalues well-grouped around 1 and that it could be solved very efficiently by the conjugate gradient method, using the FFT to perform the matrix-vector multiplications in  $O(N \log N)$ . Widlund [Wid] first explained the favorable grouping of the eigenvalues by showing that the inner linear system was in fact the discretization of the identity plus a compact operator. Wegmann [Weg2] expressed this operator in terms of the conjugation operator for the disk and gave further theoretical discussion.

For our extension of Fornberg's method to circular domains, we need to extend both the analyticity conditions and the linearization. The analyticity conditions for the multi-disk case are given below in Theorem 5 in terms of Fourier series and are considerably more complicated than the single-disk case. In addition, for Newton's method, we must now linearize about both the boundary correspondences and the centers and radii of the disks. Applying the analyticity conditions to the linearizations leads to our inner linear system for the Newton updates.

Fornberg's method [Fo] has been extended in a similar fashion to the exterior disk, ellipse, cross-shaped, and annular regions in [DE, DEP, DP]. In all these cases, it has been shown that the inner linear systems are discretizations of the identity plus a compact operator involving the conjugation

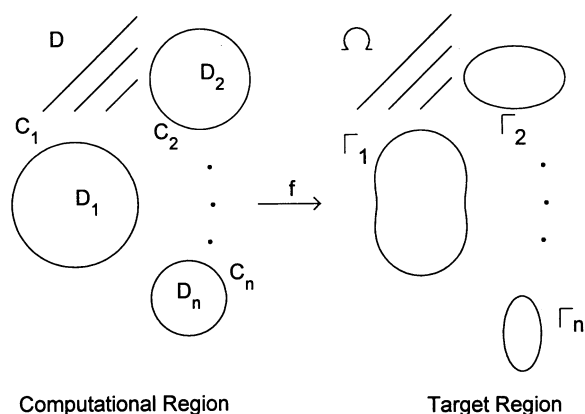


Fig. 1. Computational and target regions

operator, so that the conjugate gradient method works efficiently and FFTs may be used. However, as the ellipse, cross, or annulus gets thinner ( $\rho \rightarrow 1$ ), the operators get “less compact”, the eigenvalues spread, and the number of conjugate gradient iterations increases. In the present case of the circle map, as the reader will see below, it appears that both the compactness of the underlying operators and the fast matrix-vector multiplication are lost. The conjugate gradient method may still be used with more iterations and a cost of  $O(N^2)$ . We presently have limited theoretical explanation of our observations. In this sense, our method is in the same state as Fornberg’s original method was in 1980, before Widlund first explained its behaviour. Wegmann has developed similar methods for the disk, ellipse, and annulus in a series of papers [Weg1, Weg2, Weg3, Weg4, Weg5].

The paper begins in Sect. 2 with a description of the circle map problem and the setting of an appropriate normalization at infinity. The analyticity conditions that are the basis of the Fornberg-like mapping methods are explained and described for our multiply connected circle mappings in Sect. 3. In Sect. 4, we describe explicitly the linearizations needed for constructing circle maps for triply connected domains. In Sect. 5, we combine the linearizations and analyticity conditions to form a discrete linear system for the Newton step. We give numerical examples in Sect. 6. Additional background information on some specific numerical conformal mapping methods related to this work is given in remarks at the end of the paper.

## 2. The circle map

Figure 1 explains the geometry and notation used in this paper. We are seeking a conformal map  $f$  from the complement,  $D$ , of  $n$  closed nonintersecting disks,  $D_k$ ,  $1 \leq k \leq n$ , onto a region  $\Omega$  which is exterior to  $n$  smooth Jordan

curves,  $\Gamma_k$ ,  $1 \leq k \leq n$ . The curves  $\Gamma_k$  and their interiors are nonintersecting.  $n$  is the *connectivity* of the  $\Omega$  and  $D$ . We assume that  $n \geq 2$ . In particular, we have

$$\overline{D}^c = \cup_{k=1}^{k=n} D_k$$

The circular disks  $D_k$  have boundaries  $C_k$  with centers  $z_k$  and radii  $\rho_k$ ,  $1 \leq k \leq n$ . The boundary of  $D$  is  $C = C_1 + \dots + C_n$ , and the boundary of  $\Omega$  is  $\Gamma = \Gamma_1 + \dots + \Gamma_n$ .

The existence of such a map has been known for many years. In Theorem 1, we state a version of such an existence theorem taken from [He]; see also [Go].

**Theorem 1.** *Let  $\Omega$  be a region of connectivity  $n \geq 2$  in the extended complex plane such that  $\infty \in \Omega$ . Then there exists a unique circular region  $D$  of connectivity  $n$  and a unique one-to-one analytic function  $g$  in  $\Omega$  satisfying the normalization*

$$(1) \quad g(z) = z + O(1/z)$$

such that  $g(\Omega) = D$ .

It should be stressed that we are finding the map from  $D$  to  $\Omega$  which would be  $f = g^{-1}$  in the above theorem. The important point to be made is that Theorem 1 states that region  $D$  is uniquely determined. That is, all centers and radii are determined. Thus the circle map problem consists of finding the conformal map (subject to the normalization at  $\infty$ ) and finding the centers and radii of  $D$ . Finding the boundary correspondence is equivalent to finding  $f$ . Assume  $\Gamma_k$  is parameterized by  $\Gamma_k : \gamma_k(S)$  where  $S$  is arclength. The circle map problem is defined as follows:

#### *Circle map problem*

Determine the circle region  $D$  with centers  $z_k$  and radii  $\rho_k$  and the boundary correspondences  $S_k(\theta)$  such that

$$f(z_k + \rho_k e^{i\theta}) := \gamma_k(S_k(\theta))$$

extends as an analytic function into  $D$  with normalization at  $\infty$  given by

$$f(z) = z + O(1/z).$$

We find it convenient to employ a different normalization at  $\infty$  than the one given in (1). Consider Theorem 2 taken from [Go, p. 234].

**Theorem 2.** *Every function that maps a circular domain  $D$  univalently onto another circular domain  $D'$  is a linear fractional transformation.*

Thus the univalent function mapping a circle domain  $D$  to a circle domain  $D'$  and mapping  $\infty$  to  $\infty$  is actually linear. Our normalization relaxes (1) to

$$(2) \quad f(z) = Az + B + O(1/z)$$

where  $A \neq 0$  and  $B$  are two complex constants to be determined. We fix centers  $z_1$  and  $z_2$  of the circle domain which then determines  $A$  and  $B$ .

If  $\Gamma$  is sufficiently smooth so that  $f$  extends smoothly to the boundary then we may write

$$f(z) = Az + B + \frac{1}{2\pi i} \int_C \frac{f(\zeta)}{\zeta - z} d\zeta$$

where  $C = C_1 + C_2 + \dots + C_n$  and

$$\frac{1}{2\pi i} \int_{C_k} \frac{f(\zeta)}{z - \zeta} d\zeta = \sum_{j=1}^{\infty} a_{k,-j} \left( \frac{\rho_k}{z - z_k} \right)^j.$$

Substituting these values we obtain a useful computational form of the map:

$$(3) \quad f(z) = Az + B + \sum_{k=1}^n \sum_{j=1}^{\infty} a_{k,-j} \left( \frac{\rho_k}{z - z_k} \right)^j.$$

### 3. Analyticity conditions

We are concerned with finding conditions for analytically extending functions from  $C := \partial D$  into  $D$ . The ideas presented are similar to [He, Sect. 14.3, DE, DEP, DP]. Theorem 3 is a statement for general regions  $D$  in Figure 1 and will be applied later to circle regions.

**Theorem 3.** *Let  $D$  be a region of connectivity  $n \geq 2$  in the extended complex plane. Also, let  $h \in \text{Lip}(C)$ . Then the following two statements are equivalent:*

(i)  *$h$  extends to an analytic function  $f(z)$  in  $D/\{\infty\}$  where*

$$f(z) = Az + B + O(1/z), \quad A \neq 0, \quad |z| \approx \infty.$$

(ii) *For any  $z_1$  in  $D_1$  we have*

$$\int_C \frac{h(\zeta)}{(\zeta - z_1)^2} d\zeta \neq 0 \quad \text{and} \quad \int_C \frac{h(\zeta)}{(\zeta - z_1)^2(\zeta - z)} d\zeta = 0, \quad z \in \overline{D}^c.$$

*Proof.* First we show that (i) implies (ii). By assumption we have

$$h(\zeta) = f^+(\zeta) = \lim_{z \rightarrow \zeta} f(z) \quad z \in D, \quad \zeta \in C,$$

where  $f$  is analytic in  $D/\{\infty\}$  with  $f(z) = Az + B + O(1/z)$ ,  $|z| \approx \infty$ ,  $A \neq 0$ . Fix  $z_1 \in D_1$  and define  $F(z) := f(z)/(z - z_1)^2$  for  $z \in D/\{\infty\}$ . It is easy to see that the conditions on  $f$  imply that  $F$  is analytic in  $D$  with a removable singularity at  $z = \infty$ . Moreover, we have

$$F^+(\zeta) = \frac{f^+(\zeta)}{(\zeta - z_1)^2} = \frac{h(\zeta)}{(\zeta - z_1)^2}.$$

It follows that  $F^+(\zeta)$  represents the boundary values of a function  $F(z)$  which is analytic in  $D$ . Furthermore, for  $z \in \overline{D}^c$ , the mapping  $\zeta \rightarrow (\zeta - z)^{-1}F(\zeta)$  is analytic in  $D$  and continuous on  $D \cup C$ . Hence

$$0 = \int_C \frac{F^+(\zeta)d\zeta}{(\zeta - z)} = \int_C \frac{h(\zeta)d\zeta}{(\zeta - z_1)^2(\zeta - z)}, \quad z \in \overline{D}^c.$$

This proves the second part of (ii).

The first part of (ii) requires some general derivations that we begin now. Since  $F$  has a removable singularity at  $z = \infty$  we may write

$$F(z) = \sum_{j=1}^{\infty} \frac{F_j}{(z - z_1)^j}, \quad |z| \approx \infty.$$

Then applying Cauchy's Theorem for  $z \in D$  we obtain

$$\begin{aligned} F(z) &= \frac{1}{2\pi i} \int_C \frac{F^+(\zeta)}{(\zeta - z)} d\zeta \\ &= \frac{1}{2\pi i} \int_C \frac{h(\zeta)d\zeta}{(\zeta - z_1)^2(\zeta - z)} \\ &= -\frac{1}{2\pi i} \frac{1}{(z - z_1)} \int_C \frac{h(\zeta)d\zeta}{(\zeta - z_1)^2 \left(1 - \frac{\zeta - z_1}{z - z_1}\right)} \\ &= -\frac{1}{2\pi i} \frac{1}{(z - z_1)} \int_C \frac{h(\zeta)}{(\zeta - z_1)^2} \sum_{j=0}^{\infty} \left(\frac{\zeta - z_1}{z - z_1}\right)^j d\zeta \\ &= \sum_{j=1}^{\infty} (z - z_1)^{-j} \left( -\frac{1}{2\pi i} \int_C \frac{h(\zeta)d\zeta}{(\zeta - z_1)^{-j+3}} \right). \end{aligned}$$

Comparing coefficients shows us that

$$F_j = -\frac{1}{2\pi i} \int_C \frac{h(\zeta)d\zeta}{(\zeta - z_1)^{-j+3}}, \quad j \geq 1.$$

Finally, we obtain for  $|z| \approx \infty$

$$Az + B + O(1/z) = f(z) = (z - z_1)^2 F(z),$$

which, by the assumptions on  $A$  in part (i), implies

$$0 \neq A = F_1 = -\frac{1}{2\pi i} \int_C \frac{h(\zeta)}{(\zeta - z_1)^2} d\zeta.$$

This establishes the first part of (ii).

Next we show that (ii) implies (i). To this end fix  $z_1 \in D_1$  and for  $z \in \overline{D}^c$  define

$$F(z) := \int_C \frac{h(\zeta)}{(\zeta - z_1)^2(\zeta - z)} d\zeta$$

Also, set  $F(z) = 0$  for  $z \in D$ . Fix  $\zeta \in C_k$  for some  $1 \leq k \leq n$  and define

$$F_k(z) := \frac{1}{2\pi i} \int_{C_k} \frac{h(\zeta)}{(\zeta - z_1)^2(\zeta - z)} d\zeta$$

so that

$$F_1(z) + F_2(z) + \dots + F_n(z) = F(z) = 0, \quad z \in \overline{D}^c.$$

Then Sokhotskyi's formula applied to  $C_k$ , and the continuity of  $F_j(z)$  on  $C_k, j \neq k$ , gives us

$$\begin{aligned} \frac{h(\zeta)}{(\zeta - z_1)^2} &= F_k^+(\zeta) - F_k^-(z) \\ &= F_k^+(\zeta) + F_1^-(z) + \dots + F_{k-1}^-(z) + F_{k+1}^-(z) + \dots + F_n^-(z) \\ &= F_k^+(\zeta) + F_1^+(\zeta) + \dots + F_{k-1}^+(\zeta) + F_{k+1}^+(\zeta) + \dots + F_n^+(\zeta) \\ &= F^+(\zeta) \end{aligned}$$

where

$$F_k^+(\zeta) := \lim_{\substack{z \rightarrow \zeta \\ z \in D_k}} F_k(z) \quad F_k^-(z) := \lim_{\substack{z \rightarrow \zeta \\ z \in (\overline{D}_k)^c}} F_k(z)$$

That is,  $F(z)$  is analytic in  $D$  with boundary function  $h(\zeta)/(\zeta - z_1)^2$ . Moreover, it is clear that  $F(\infty) = 0$ . We may then expand  $F$  so that

$$F(z) = \sum_{j=1}^{\infty} \frac{F_j}{(z - z_1)^j}, \quad |z| \approx \infty,$$

where

$$F_j = -\frac{1}{2\pi i} \int_C \frac{h(\zeta)d\zeta}{(\zeta - z_1)^{-j+3}}.$$

Now define  $f(z) := (z - z_1)^2 F(z)$ . Then for  $|z|$  large we have

$$f(z) = \sum_{j=1}^{\infty} \frac{F_j}{(\zeta - z_1)^{j-2}} = F_1(z - z_1) + F_2 + \frac{F_3}{(z - z_1)} + \dots$$

Noting that

$$f^+(\zeta) = (\zeta - z_1)^2 F^+(\zeta) = h(\zeta)$$

it is easy to see that  $f$  is the desired function satisfying all the conditions in (i). That is,  $f$  is the analytic extension of  $h$  to  $D/\{\infty\}$ .  $\square$

The following corollary is an immediate consequence of Theorem 3 and is useful in the derivation of the analyticity conditions in Theorem 5. Note that, since the disks  $D_k$  are uniquely determined by the Jordan curves  $\Gamma_k$  according to Theorem 1, it clearly does not matter which curve is labeled  $\Gamma_1$ . However, once  $\Gamma_1$  is specified  $D_1$  and  $z_1$  are kept fixed.

**Corollary 4.**  $h \in \text{Lip}(C)$  extends to an analytic function in  $D$  satisfying the condition in equation (2) if and only if for any  $z_k \in D_k$

$$\int_{\partial D} \frac{h(\zeta)}{(\zeta - z_1)^2} d\zeta \neq 0, \quad \int_{\partial D} \frac{h(\zeta)}{(\zeta - z_1)^2(\zeta - z_k)^j} d\zeta = 0, \\ j \geq 1, \quad 1 \leq k \leq n.$$

*Proof.* Fix  $z_k$  in  $D_k$ . It is enough to establish the result in a ball centered at  $z_k$  and contained in  $D_k$ . For  $\zeta \in C_k$  choose any  $z \in \overline{D}^c$  such that

$$\left| \frac{z - z_k}{\zeta - z_k} \right| < 1.$$

Then we have

$$0 = \int_C \frac{h(\zeta)}{(\zeta - z_1)^2(\zeta - z)} d\zeta = \int_C \frac{h(\zeta)}{(\zeta - z_1)^2} \frac{1}{(\zeta - z_k)} \sum_{j=0}^{\infty} \left( \frac{z - z_k}{\zeta - z_k} \right)^j d\zeta$$

if and only if

$$0 = \int_C \frac{h(\zeta)}{(\zeta - z_1)^2(\zeta - z_k)^j} d\zeta, \quad j \geq 1. \quad \square$$

We are now in a position to derive analyticity conditions for the disk map. To avoid notational complexity, derivations will only be made for the

3 disk case. Extensions to  $n$  disks are straight forward. We have need of the binomial coefficients  $B_k$  given by

$$\frac{1}{(1 - \Delta)^k} = \sum_{j=0}^{\infty} B_{kj} \Delta^j, \quad |\Delta| < 1,$$

$$B_{kj} = \frac{k(k+1) \cdots (k+j-1)}{j!}, \quad k \geq 1, \quad j \geq 0.$$

If we now apply this to the integrals given in Corollary 4 ( $1 \leq k \leq 3$ ), then the following identities will result for  $j \geq 1$ :

$$k = 1$$

$$\int_{C_1} \frac{f(\zeta) d\zeta}{(\zeta - z_1)^{j+2}} = \frac{2\pi i}{\rho_1^{j+1}} a_{1,j+1}$$

$$\int_{C_2} \frac{f(\zeta) d\zeta}{(\zeta - z_1)^{j+2}} = \frac{2\pi i \rho_2}{(z_2 - z_1)^{j+2}} \sum_{\nu=0}^{\infty} B_{j+2,\nu} \left( \frac{\rho_2}{z_1 - z_2} \right)^{\nu} a_{2,-\nu-1}$$

$$\int_{C_3} \frac{f(\zeta) d\zeta}{(\zeta - z_1)^{j+2}} = \frac{2\pi i \rho_3}{(z_3 - z_1)^{j+2}} \sum_{\nu=0}^{\infty} B_{j+2,\nu} \left( \frac{\rho_3}{z_1 - z_3} \right)^{\nu} a_{3,-\nu-1}$$

$$k = 2$$

$$\int_{C_1} \frac{f(\zeta) d\zeta}{(\zeta - z_1)^2 (\zeta - z_2)^j} = \frac{2\pi i}{\rho_1 (z_1 - z_2)^j} \sum_{\nu=0}^{\infty} B_{j\nu} \left( \frac{\rho_1}{z_2 - z_1} \right)^{\nu} a_{1,-\nu+1}$$

$$\int_{C_2} \frac{f(\zeta) d\zeta}{(\zeta - z_1)^2 (\zeta - z_2)^j} = \frac{2\pi i \rho_2^{-j+1}}{(z_2 - z_1)^2} \sum_{\nu=0}^{\infty} B_{2\nu} \left( \frac{\rho_2}{z_1 - z_2} \right)^{\nu} a_{2,j-\nu-1}$$

$$\int_{C_3} \frac{f(\zeta) d\zeta}{(\zeta - z_1)^2 (\zeta - z_2)^j} = \frac{2\pi i \rho_3 (z_3 - z_1)^{-2}}{(z_3 - z_2)^j} \sum_{\nu=0}^{\infty} \sum_{l=0}^{\infty} B_{2\nu} \left( \frac{\rho_3}{z_1 - z_3} \right)^{\nu} \\ \times B_{j\nu} \left( \frac{\rho_3}{z_2 - z_3} \right)^l a_{3,-\nu-l-1}$$

$$k = 3$$

$$\int_{C_1} \frac{f(\zeta)d\zeta}{(\zeta - z_1)^2(\zeta - z_3)^j} = \frac{2\pi i}{\rho_1(z_1 - z_3)^j} \sum_{\nu=0}^{\infty} B_{j\nu} \left( \frac{\rho_1}{z_3 - z_1} \right)^{\nu} a_{1,-\nu+1}$$

$$\int_{C_2} \frac{f(\zeta)d\zeta}{(\zeta - z_1)^2(\zeta - z_3)^j} = \frac{2\pi i \rho_2(z_2 - z_1)^{-2}}{(z_2 - z_3)^j} \sum_{\nu=0}^{\infty} \sum_{l=0}^{\infty} B_{2\nu} \left( \frac{\rho_2}{z_1 - z_2} \right)^{\nu}$$

$$\times B_{jl} \left( \frac{\rho_2}{z_3 - z_2} \right)^l a_{2,-\nu-l-1}$$

$$\int_{C_3} \frac{f(\zeta)d\zeta}{(\zeta - z_1)^2(\zeta - z_3)^j} = \frac{2\pi i \rho_3^{-j+1}}{(z_3 - z_1)^2} \sum_{\nu=0}^{\infty} B_{2\nu} \left( \frac{\rho_3}{z_1 - z_3} \right)^{\nu} a_{3,j-\nu-1}$$

Now using  $C = C_1 + C_2 + C_3$  and setting

$$\int_C \frac{h(\zeta)}{(\zeta - z_1)^2(\zeta - z_k)^j} d\zeta = 0, \quad 1 \leq k \leq 3$$

we obtain the following theorem.

**Theorem 5.** *Let  $D$  be the exterior circular region to the disks  $D_k : z_k + \rho_k e^{i\theta}, 1 \leq k \leq 3$ . Suppose  $f \in \text{Lip}(C)$  has the Fourier series representation*

$$f(z_k + \rho_k e^{i\theta}) = \sum_{j=-\infty}^{\infty} a_{kj} e^{ij\theta}, \quad 1 \leq k \leq 3.$$

*Then  $f$  extends analytically into  $D$  if and only if for  $j \geq 1$*

$$k = 1$$

$$0 = a_{1,j+1} - \left( \frac{\rho_1}{z_2 - z_1} \right)^{j+1} \sum_{\nu=0}^{\infty} B_{j+2,\nu} \left( \frac{\rho_2}{z_1 - z_2} \right)^{\nu+1} a_{2,-\nu-1}$$

$$- \left( \frac{\rho_1}{z_3 - z_1} \right)^{j+1} \sum_{\nu=0}^{\infty} B_{j+2,\nu} \left( \frac{\rho_3}{z_1 - z_3} \right)^{\nu+1} a_{3,-\nu-1}$$

$$k = 2$$

$$0 = - \left( \frac{\rho_2}{z_1 - z_2} \right)^{j-1} \sum_{\nu=0}^{\infty} B_{j\nu} \left( \frac{\rho_1}{z_2 - z_1} \right)^{\nu-1} a_{1,-\nu+1}$$

$$+ \sum_{\nu=0}^{\infty} B_{2\nu} \left( \frac{\rho_2}{z_1 - z_2} \right)^{\nu} a_{2,j-\nu-1}$$

$$\begin{aligned}
 & - \left( \frac{z_2 - z_1}{z_3 - z_1} \right)^2 \left( \frac{\rho_2}{z_3 - z_2} \right)^{j-1} \sum_{l,\nu=0}^{\infty} B_{2\nu} B_{jl} \\
 & \left( \frac{\rho_3}{z_1 - z_3} \right)^{\nu} \left( \frac{\rho_3}{z_2 - z_3} \right)^{l+1} a_{3,-\nu-l-1} \\
 & \qquad \qquad \qquad k = 3 \\
 0 = & - \left( \frac{\rho_3}{z_1 - z_3} \right)^{j-1} \sum_{\nu=0}^{\infty} B_{j\nu} \left( \frac{\rho_1}{z_3 - z_1} \right)^{\nu-1} a_{1,-\nu+1} \\
 & - \left( \frac{z_3 - z_1}{z_2 - z_1} \right)^2 \left( \frac{\rho_3}{z_2 - z_3} \right)^{j-1} \sum_{l,\nu=0}^{\infty} B_{2\nu} B_{jl} \\
 & \left( \frac{\rho_2}{z_1 - z_2} \right)^{\nu} \left( \frac{\rho_2}{z_3 - z_2} \right)^{l+1} a_{2,-\nu-l-1} \\
 & + \sum_{\nu=0}^{\infty} B_{2\nu} \left( \frac{\rho_3}{z_1 - z_3} \right)^{\nu} a_{3,j-\nu-1}
 \end{aligned}$$

To obtain the form given in Theorem 5 some minor scaling and index shifting is applied to the identities for  $k = 1, 2, 3$ . This is done for convenience and stability in computations. Also, to see the exact equations used for 2 disks just delete any term containing a  $z_3$  or a  $\rho_3$ . This results in deleting the last part of the first two equations and entirely deleting the last equation. The reader will note the symmetries for extending to arbitrary  $n$  disks. The main complication arises in going from the 2 to 3 disks, since double sums are needed for integration and expansion about the second and third disks when  $z_1$  is in the first disk.

**4. Linearizations**

We seek linearizations for the circle map (in particular for 3 circles). We remind the reader that we are using the normalization

$$(4) \qquad f(z) = Az + B + O(1/z)$$

where  $A \neq 0$  and  $B$  are to be determined from fixing the centers  $z_1$  and  $z_2$ . This leaves us with the problem of finding the radii  $\rho_1, \rho_2, \rho_3$ , and the center  $z_3$ .

Recall that, for the exact map  $f$ , our boundary correspondence would satisfy

$$f(z_k + \rho_k e^{i\theta}) = \gamma_k(S_k(\theta)) \quad 1 \leq k \leq 3.$$

The following process is to be applied at the  $m$ th Newton step but the notation indicating this will be suppressed to avoid confusion. As usual, we make the guess to  $S_k(\theta)$  and correct with the real,  $2\pi$ -periodic function  $U_k(\theta)$ . If  $S_k$  is arclength this leads to

$$\gamma_k(S_k(\theta) + U_k(\theta)) \approx \xi_k(\theta) + e^{i\beta_k(\theta)}U_k(\theta), \quad 1 \leq k \leq 3$$

where

$$\xi_k(\theta) := \gamma_k(S_k(\theta)) \quad \beta_k(\theta) := \arg \gamma'(S_k(\theta)).$$

Linearizations for the radii  $\rho_1, \rho_2, \rho_3$  and the center  $z_3$  are carried out in a manner similar to the annulus map [LM, DP]. In fact, we use

$$\begin{aligned} f(z_1 + (\rho_1 + \delta\rho_1)e^{i\theta}) &\approx f(z_1 + \rho_1e^{i\theta}) \\ &\quad + f'(z_1 + \rho_1e^{i\theta})(\delta\rho_1e^{i\theta}) \\ f(z_2 + (\rho_2 + \delta\rho_2)e^{i\theta}) &\approx f(z_2 + \rho_2e^{i\theta}) \\ &\quad + f'(z_2 + \rho_2e^{i\theta})(\delta\rho_2e^{i\theta}) \\ f(z_3 + \delta z_3 + (\rho_3 + \delta\rho_3)e^{i\theta}) &\approx f(z_3 + \rho_3e^{i\theta}) \\ &\quad + f'(z_3 + \rho_3e^{i\theta})(\delta z_3 + \delta\rho_3e^{i\theta}). \end{aligned}$$

As in the annulus case, we also use

$$\zeta_k(\theta) := f'(z_k + \rho_k e^{i\theta}) e^{i\theta} = -i\rho_k^{-1} e^{i\beta_k(\theta)} S'_k(\theta).$$

In summary, equating the linearized terms we seek to find the corrections  $U_1, U_2, U_3, \delta\rho_1, \delta\rho_2, \delta\rho_3, \delta z_3$  such that  $f$  extends as an analytic function into the circle region  $D$  where  $f$  is defined on  $C$  by

$$\begin{aligned} f(z_1 + \rho_1 e^{i\theta}) &:= \xi_1(\theta) + e^{i\beta_1(\theta)}U_1(\theta) - \zeta_1(\theta)\delta\rho_1 \\ (5) \quad f(z_2 + \rho_2 e^{i\theta}) &:= \xi_2(\theta) + e^{i\beta_2(\theta)}U_2(\theta) - \zeta_2(\theta)\delta\rho_2 \\ f(z_3 + \rho_3 e^{i\theta}) &:= \xi_3(\theta) + e^{i\beta_3(\theta)}U_3(\theta) - \zeta_3(\theta)(\delta\rho_3 + \delta z_3/e^{i\theta}). \end{aligned}$$

## 5. Discretizations

For  $1 \leq k \leq 3, 1 \leq j, l \leq N$ , we define the  $N$ -vectors and  $N \times N$  matrices:

$$\begin{aligned} F &:= [w^{-jl}] = \text{FFT matrix} \\ E_k &:= \text{diag}_j(e^{i\beta_k(\theta_j)}) \end{aligned}$$

$$\begin{aligned}
 \dot{\underline{S}}_k &:= \frac{N}{2\pi} [S_k(\theta_{j+1}) - S_k(\theta_j)] \\
 \underline{U}_k &:= [U_k(\theta_j)] \\
 \underline{\xi}_k &:= [\gamma_k(S_k(\theta_j))] \\
 \underline{\zeta}_k &:= i\rho_k^{-1} E_k \dot{\underline{S}}_k \\
 \underline{f}_k &:= \left[ f \left( z_k + \rho_k e^{i\theta_j} \right) \right] \\
 \underline{a}_k &:= \frac{1}{N} F \underline{f}_k \\
 \underline{z} &:= \left[ e^{-i\theta_j} \right].
 \end{aligned}
 \tag{6}$$

From (5) our discrete system can then be written as

$$\begin{aligned}
 N\underline{a}_1 &= F\underline{f}_1 = F\underline{\xi}_1 + FE_1\underline{U}_1 + \delta\rho_1 F\underline{\zeta}_1 \\
 N\underline{a}_2 &= F\underline{f}_2 = F\underline{\xi}_2 + FE_2\underline{U}_2 + \delta\rho_2 F\underline{\zeta}_2 \\
 N\underline{a}_3 &= F\underline{f}_3 = F\underline{\xi}_3 + FE_3\underline{U}_3 + \delta\rho_3 F\underline{\zeta}_3 + \delta z_3 F \left( \underline{z} * \underline{\zeta}_3 \right)
 \end{aligned}
 \tag{7}$$

where  $*$  denotes Hadamard product.

Now we seek a discrete version of the analyticity conditions given in Theorem 5. Essentially, we truncate the 3 analyticity conditions to  $N/2$  terms. There are a few subtle points to be made and we will discuss them below. Thus our discrete analyticity conditions are taken as

$$k = 1$$

$$\begin{aligned}
 0 &= \hat{a}_{1,j+1} - \left( \frac{\rho_1}{z_2 - z_1} \right)^{j+1} \sum_{\nu=0}^{N/2-1} B_{j+2,\nu} \left( \frac{\rho_2}{z_1 - z_2} \right)^{\nu+1} \hat{a}_{2,-\nu-1} \\
 &\quad - \left( \frac{\rho_1}{z_3 - z_1} \right)^{j+1} \sum_{\nu=0}^{N/2-1} B_{j+2,\nu} \left( \frac{\rho_3}{z_1 - z_3} \right)^{\nu+1} \hat{a}_{3,-\nu-1}
 \end{aligned}$$

$$k = 2$$

$$\begin{aligned}
 0 &= - \left( \frac{\rho_2}{z_1 - z_2} \right)^{j-1} \sum_{\nu=0}^{N/2-1} B_{j\nu} \left( \frac{\rho_1}{z_2 - z_1} \right)^{\nu-1} \hat{a}_{1,-\nu+1} \\
 &\quad + \sum_{\nu=0}^{N/2-1} B_{2\nu} \left( \frac{\rho_2}{z_1 - z_2} \right)^{\nu} \hat{a}_{2,j-\nu-1} \\
 &\quad - \left( \frac{z_2 - z_1}{z_3 - z_1} \right)^2 \left( \frac{\rho_2}{z_3 - z_2} \right)^{j-1} \sum_{l,\nu=0}^{N/4-1} B_{2\nu} B_{jl}
 \end{aligned}$$

$$\begin{aligned}
& \left( \frac{\rho_3}{z_1 - z_3} \right)^\nu \left( \frac{\rho_3}{z_2 - z_3} \right)^{l+1} \hat{a}_{3, -\nu-l-1} \\
& k = 3 \\
0 = & - \left( \frac{\rho_3}{z_1 - z_3} \right)^{j-1} \sum_{\nu=0}^{N/2-1} B_{j\nu} \left( \frac{\rho_1}{z_3 - z_1} \right)^{\nu-1} \hat{a}_{1, -\nu+1} \\
& - \left( \frac{z_3 - z_1}{z_2 - z_1} \right)^2 \left( \frac{\rho_3}{z_2 - z_3} \right)^{j-1} \sum_{l,\nu=0}^{N/4-1} B_{2\nu} B_{jl} \\
& \left( \frac{\rho_2}{z_1 - z_2} \right)^\nu \left( \frac{\rho_2}{z_3 - z_2} \right)^{l+1} \hat{a}_{2, -\nu-l-1} \\
& + \sum_{\nu=0}^{N/2-1} B_{2,\nu} \left( \frac{\rho_3}{z_1 - z_3} \right)^\nu \hat{a}_{3, j-\nu-1}
\end{aligned}$$

where  $0 \leq j \leq N/2$ . For  $N$  large we expect nearly negligible contributions from higher numbered Fourier coefficients. Thus any term falling outside of  $-N/2 - 1 \leq j \leq N/2$  we assume to be 0 instead of using conflicting information between analyticity and  $N$ -periodicity of the discrete Fourier coefficients. In particular, in the first equation we impose  $\hat{a}_{1, N/2+1} = 0$  and  $\hat{a}_{1, -N/2} = 0$ . Moreover, our double sums are taken to range only from  $0 \leq \nu \leq N/4 - 1$  to stay within the desired range of indices.

Another important point to be made is the growth of binomial coefficients. One cannot simply compute binomial coefficients for large  $N$  due to overflow. Instead, we observe that each term containing binomial coefficients has geometric decay as well. Therefore care must be taken in organizing the computations so that geometric growth kills off binomial growth. This is the reason for the scaling and index shifting of the equations in Theorem 5.

It is important that the sums be done efficiently, since they make up the matrix-vector multiplications in the conjugate gradient iterations described below. By summing with respect to  $\nu$  first, the double sums can be treated as 2 matrix-vector multiplications and computed in  $O(N^2)$  operations. (The  $\nu$  sum can be computed in  $O(N \log N)$  as a Hankel matrix multiplication, but we have not done this. In future work, we hope to simplify the analyticity conditions.)

We will suppress many details which can be found in [Ho]. We just note that with appropriate  $3N/2 \times N$  matrices  $P_1, P_2, P_3$ , our discrete system takes the form

$$(8) \quad \underline{0} = [P_1 \ P_2 \ P_3] \begin{bmatrix} \underline{a}_1 \\ \underline{a}_2 \\ \underline{a}_3 \end{bmatrix}.$$

Substituting (7) into (8) and rearranging we obtain

$$(9) \quad P_1 \left( FE_1 \underline{U}_1 + \delta\rho_1 F \underline{\zeta}_1 \right) + P_2 \left( FE_2 \underline{U}_2 + \delta\rho_2 F \underline{\zeta}_2 \right) \\ + P_3 \left( FE_3 \underline{U}_3 + \delta\rho_3 F \underline{\zeta}_3 + F(z * \underline{\zeta}_3) \right) (\text{Re}\delta z_3 + i\text{Im}\delta z_3) = \underline{g}$$

where

$$(10) \quad \underline{g} := - [P_1 \ P_2 \ P_3] \begin{bmatrix} F \underline{\zeta}_1 \\ F \underline{\zeta}_2 \\ F \underline{\zeta}_3 \end{bmatrix}.$$

If we define the  $3N/2$  vectors

$$(11) \quad \underline{w}_k = P_k F \underline{\zeta}_k, \quad \underline{w}_{z_3} = P_3 F (z * \underline{\zeta}_3)$$

and put

$$(12) \quad P = [P_1 \ P_2 \ P_3], \quad W = [\underline{w}_1 \ \underline{w}_2 \ \underline{w}_3 \ \underline{w}_{z_3} \ i\underline{w}_{z_3}]$$

as well as

$$\underline{U} = \begin{bmatrix} \underline{U}_1 \\ \underline{U}_2 \\ \underline{U}_3 \\ \delta\rho_1 \\ \delta\rho_2 \\ \delta\rho_3 \\ \text{Re}\delta z_3 \\ \text{Im}\delta z_3 \end{bmatrix}$$

then our system becomes

$$(13) \quad D\underline{U} := [P \ W] \begin{bmatrix} F & 0 & 0 & 0 \\ 0 & F & 0 & 0 \\ 0 & 0 & F & 0 \\ 0 & 0 & 0 & I \end{bmatrix} \begin{bmatrix} E_1 & 0 & 0 & 0 \\ 0 & E_2 & 0 & 0 \\ 0 & 0 & E_3 & 0 \\ 0 & 0 & 0 & I \end{bmatrix} \underline{U} = \underline{g}.$$

Taking normal equations and using the fact that  $\underline{U}$  is real gives us

$$(14) \quad \frac{2}{N} \text{Re} (D^H D) \underline{U} = \frac{2}{N} \text{Re} (D^H \underline{g}).$$

Note that  $\frac{2}{N} \text{Re}(D^H D)$  is positive semi-definite so that we can use the conjugate gradient method. Also, we observe that the eigenvalues are grouped around 1 (but not always well grouped).

All normalization conditions are absorbed in fixing centers  $z_1$  and  $z_2$  so that (14) need not be modified. After finding the corrections, the update equations at the  $m$ th Newton step are given by

$$(15) \quad \begin{aligned} \underline{S}_k^{(m+1)} &= \underline{S}_k^{(m)} + \underline{U}_k^{(m)} \\ \rho_k^{(m+1)} &= \rho_k^{(m)} + \delta\rho_k^{(m)} \\ z_3^{(m+1)} &= z_3^{(m)} + \delta z_3^{(m)} \end{aligned}$$

for  $1 \leq k \leq 3$ .

## 6. Numerical examples

In this section we will discuss several numerical examples for the 2 and 3 disk cases. The quadratic convergence of the outer (Newton) steps, the number of conjugate gradient steps and the eigenvalue clustering of the inner linear system, and the discretization error are studied. Eigenvalue computations were performed on an IBM ES9121 Model 440 mainframe computer while other table data was taken from a Pentium PC using Fortran and Matlab.

In the tables, NFFT denotes the number of Fourier points, NN denotes the current outer Newton step, and NCGM denotes the number of conjugate gradient (CGM) steps taken. Often it is not beneficial to let CGM run until some tolerance is reached. Instead we implement a type of restart CGM in which 20 to 40 CGM steps are taken for each Newton step. In most examples, the algorithm converges to a discrete solution in less than 20 Newton steps. To study quadratic convergence we need data for  $\|U_k\|_\infty = \max_j |U_k(\theta_j)|$ ,  $|\delta\rho_k|$ , and  $|\delta z_3|$  (3 disk case).

In each example we will state the initial guess taken to start the procedure. Generally NS=1000 points on the boundaries are fitted with a periodic cubic spline parametrized by (chordal) arc length [HK]. The initial guess for the boundary correspondences is given by NFFT points along each curve equally distributed in arc length. We also need to initialize  $\rho_k$  and  $z_3$  (3 disk case). As is typical for Fornberg-like methods, a sufficiently good initial guess is required.  $z_1$  and  $z_2$  are fixed in both the 2 and 3 disk case. We fix  $z_1 = 0$  for all examples and only state the  $z_2$  chosen.

From [DP] we know that the conformal modulus of the annulus  $\rho$  plays a key role in the algorithm. In particular, the governing equations have a tighter spectrum clustering for smaller  $\rho$  so that CGM converges rapidly. We will see in the examples to follow that the radii  $\rho_k$  and centers  $z_k$  for the circle map also play a key role in convergence. This can be expected from the equations given in Theorem 5. Smaller radii and farther separated disks

make the geometric decay better. In fact, as

$$\left| \frac{\rho_k}{z_j - z_k} \right| \rightarrow 1$$

the eigenvalues of  $\frac{2}{\text{NFFT}} \text{Re}(D^H D)$  are less well grouped around 1. This means more CGM iterations are required to reach a fixed tolerance in the inner linear systems.

For the graphics, we plot images of equally spaced horizontal and vertical lines from the  $z$ -plane.

*Example (i).* This is a 2 circle test. Here we construct an exact unbounded doubly connected exterior conformal map that satisfies  $\infty \rightarrow \infty$ . This will allow us to study discrete errors and quadratic convergence for a nontrivial map. Our exact map is a composition of well-known maps. We explain all of the preliminary maps since this could be a rich source of test cases. The first map  $f_1$  is the fractional linear map

$$f_1(z) = \frac{z - a}{az - 1}$$

which is illustrated in [Gr, p. 1279]. It maps a 2 circle region to the annulus where

$$a = \frac{x_1 x_2 + 1 + \sqrt{(x_1^2 - 1)(x_2^2 - 1)}}{x_1 + x_2}$$

$$R = \frac{x_1 x_2 - 1 - \sqrt{(x_1^2 - 1)(x_2^2 - 1)}}{x_1 - x_2}$$

and  $1 < x_2 < x_1$ . The second map  $f_2$  is a scaling map

$$f_2(z) = \beta z.$$

The goal is to make  $\beta R \gg 1$  so that the region is not so extreme. The next map is the familiar Joukowski map

$$f_3(z) = z + 1/z$$

which takes the annulus from  $f_2$  onto another bounded, doubly connected region. The fourth map  $f_4$  is another scaling

$$f_4(z) = \frac{\beta}{\beta^2 + 1} z.$$

The final map  $f_5$  is the fractional linear map

$$f_5(z) = \frac{z - C}{Cz - 1}$$

**Table 1.** Discretization error for example (i)

NFFT	DISC1	DISC2
32	0.2e-08	0.3e-04
64	0.4e-11	0.1e-06
128	0.4e-11	0.6e-10

where  $C := \frac{a(\beta^2+1)}{a^2+\beta^2}$ .  $f_5$  takes the region from  $f_4$  onto the final region in Fig. 2. A simple check shows that

$$\infty \rightarrow \frac{1}{a} \rightarrow \frac{\beta}{a} \rightarrow \frac{a^2 + \beta^2}{a\beta} \rightarrow \frac{a^2 + \beta^2}{a(\beta^2 + 1)} \rightarrow \infty$$

The exact map is thus

$$f(z) = f_5(f_4(f_3(f_2(f_1(z)))))$$

We now solve the circle map problem with exact geometry  $z_1 = 0$ ,  $z_2 = 2.5$ ,  $\rho_1 = 1.0$ ,  $\rho_2 = 0.5$ . The parameter  $\beta = 25$ . Recall that in the 2 disk case only initializations for  $\rho_1$  and  $\rho_2$  are needed. The centers  $z_1$  and  $z_2$  are free parameters and so we assign them the exact values. We take the initializations  $\rho_1 = 0.9$ ,  $\rho_2 = 0.4$ . In Table 1, we list discretization errors DISC1, DISC2 at the NFFT Fourier points around each disk for NFFT=32, 64, 128. Note that  $\Gamma_2$  is the more distorted curve and hence the discretization error DISC2 is expected to be greater than DISC1 for fixed NFFT. Table 2 gives data for the outer Newton steps for NFFT = 128. We took NCGM = 25 in solving the inner linear correction system. The corrections decay quadratically until the level of discretization for this value of NFFT = 128. This is typical for Fornberg-like methods. The middle half of the  $2 \cdot \text{NFFT} + 2$  eigenvalues of the matrix in equation (14) are nearly equal to 1 and the first and last quarter of the eigenvalues decrease and increase, respectively, from 1 by about 0.5. This distribution seems to be independent of NFFT, indicating that the matrix is not the discretization of the identity plus a compact operator as in the other Fornberg-like methods. See Fig. 2 for graphics of the final map. Discrete errors are not available for the remaining examples since exact maps are not known in general.

*Example (ii).* This is a 3 circle test. Examples (ii) and (iii) should be considered together. In these examples we demonstrate the effect that the separations of the disks and the disk radii has on the numerics. Each target boundary is an ellipse generated by

$$\Gamma_k : w_k + (\cos(\theta), \alpha_k \sin(\theta)), \quad 1 \leq k \leq 3, \quad 0 \leq \theta \leq 2\pi,$$

where  $w_1 = (0.0, 0.0)$ ,  $w_2 = (10.0, 0.0)$ ,  $w_3 = (-10.0, 0.0)$ ,  $\alpha_1 = \alpha_2 = \alpha_3 = 0.6$ . Note that each ellipse is well separated from the others. This,

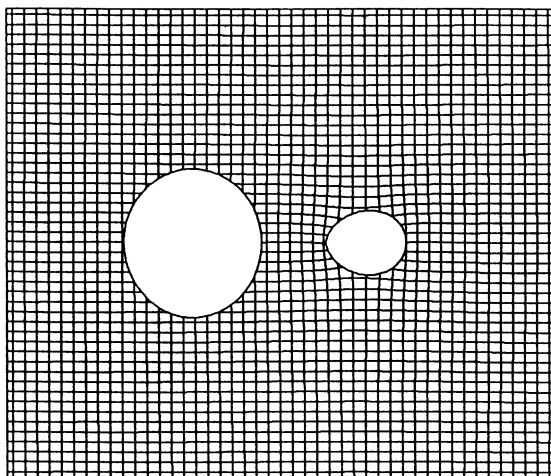


Fig. 2. Circle map for example (i)

Table 2. Newton steps for example (i). NFFT=128

NN	$ \delta\rho_1 $	$ \delta\rho_2 $	$\ U_1\ _\infty$	$\ U_2\ _\infty$
1	0.9e-01	0.8e-01	0.3e-02	0.2e-01
2	0.1e-01	0.2e-01	0.2e-02	0.3e-01
3	0.6e-03	0.1e-02	0.3e-03	0.5e-02
4	0.2e-05	0.5e-05	0.3e-05	0.9e-04
5	0.1e-08	0.2e-08	0.1e-07	0.7e-07
6	0.1e-12	0.9e-13	0.3e-11	0.2e-10
7	0.3e-17	0.1e-15	0.4e-15	0.3e-15

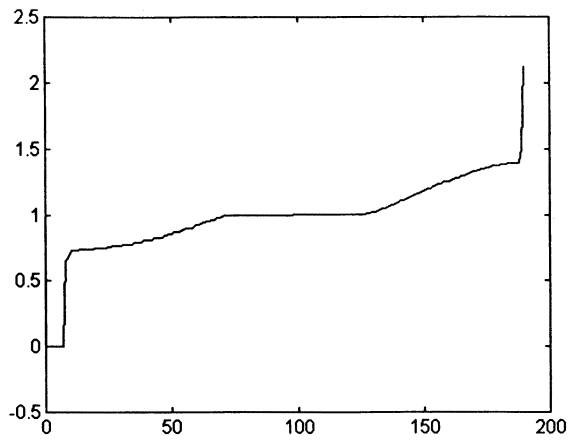
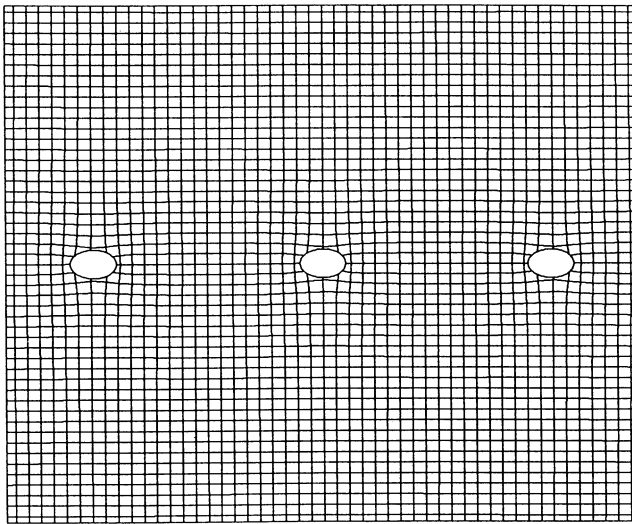
along with the relatively small circle map disk radii, make example (ii) the easier problem numerically.

We now solve the circle map problem. Here  $z_1$  and  $z_2$  are fixed to the values  $z_1 = (0.0, 0.0)$ ,  $z_2 = (10.0, 0.0)$ . We take the initializations  $\rho_1 = \rho_2 = \rho_3 = 0.7$  and  $z_3 = (-9.9, 0.0)$ . Compare to the final result of  $\rho_1 \approx 0.804540$ ,  $\rho_2 \approx 0.803569$ ,  $\rho_3 \approx 0.803569$ , and  $z_3 \approx (-10.0, 0.0)$ . In Table 3 we give data for NFFT=256. The convergence is now affected by the linearizations for  $z_3$ . Nevertheless, nearly quadratic convergence is obtained for beginning Newton steps. We took NCGM=40 per Newton step. In Fig. 3 we show an eigenvalue plot for the Newton step NN=4 corresponding to Table 3. The eigenvalues are not as well grouped as in examples (i) for the 2 disk case but CGM still converges fast. See Fig. 4 for graphics of the final map.

*Example (iii).* This is a 3 circle test to be compared to example (ii). We make the changes  $w_2 = (3.0, 0.0)$ ,  $w_3 = (-3.0, 0.0)$ , and the initializations  $\rho_1 = \rho_2 = \rho_3 = 0.75$ ,  $z_3 = (-2.9, 0.0)$ . Compare to the final values  $\rho_1 \approx$

**Table 3.** Newton steps for example (ii). NFFT=256.

NN	$ \delta\rho_1 $	$ \delta\rho_2 $	$ \delta\rho_3 $	$\ U_1\ _\infty$	$\ U_2\ _\infty$	$\ U_3\ _\infty$	$ \delta z_3 $
1	0.5e-01	0.5e-01	0.5e-01	0.8e-01	0.8e-01	0.1e-00	0.8e-01
2	0.4e-02	0.4e-02	0.3e-02	0.2e-01	0.2e-01	0.4e-01	0.2e-01
3	0.1e-03	0.1e-03	0.7e-03	0.5e-03	0.5e-03	0.4e-02	0.7e-03
4	0.2e-07	0.2e-06	0.2e-06	0.2e-05	0.2e-05	0.4e-04	0.2e-05
5	0.8e-10	0.6e-10	0.2e-09	0.8e-09	0.5e-08	0.2e-07	0.7e-08
6	0.9e-13	0.4e-12	0.9e-12	0.3e-11	0.1e-10	0.8e-10	0.2e-10
7	0.1e-15	0.1e-15	0.1e-15	0.9e-15	0.8e-14	0.2e-12	0.8e-13

**Fig. 3.** Spectrum for example (ii). NFFT=64, NN=4**Fig. 4.** Circle map for example (ii)

**Table 4.** Newton steps for example (iii). NFFT=256

NN	$ \delta\rho_1 $	$ \delta\rho_2 $	$ \delta\rho_3 $	$\ U_1\ _\infty$	$\ U_2\ _\infty$	$\ U_3\ _\infty$	$ \delta z_3 $
1	0.1e-00	0.1e-00	0.1e-00	0.5e-01	0.6e-01	0.9e-01	0.7e-01
2	0.2e-01	0.2e-01	0.2e-01	0.4e-01	0.3e-01	0.5e-01	0.3e-01
3	0.3e-03	0.2e-03	0.2e-03	0.4e-02	0.6e-02	0.1e-01	0.1e-02
4	0.5e-04	0.3e-04	0.4e-04	0.8e-03	0.5e-03	0.8e-03	0.2e-03
5	0.6e-06	0.7e-06	0.1e-05	0.1e-04	0.4e-04	0.3e-04	0.9e-05
6	0.2e-07	0.4e-07	0.8e-07	0.8e-06	0.1e-05	0.8e-05	0.8e-06
7	0.6e-08	0.2e-07	0.2e-07	0.5e-07	0.1e-06	0.2e-06	0.4e-07

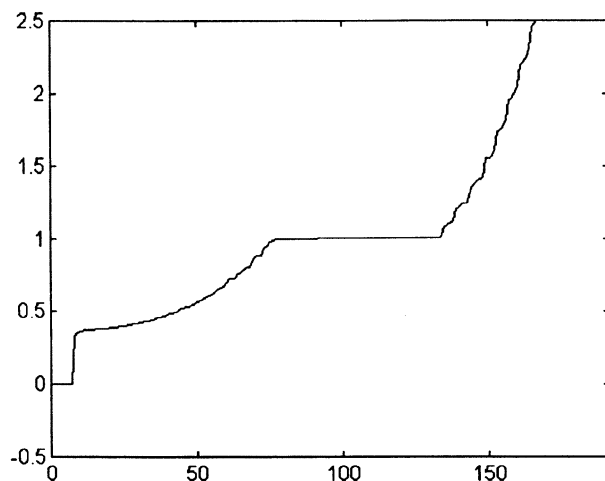


**Fig. 5.** Spectrum for example (iii). NFFT=64, NN=4

0.85986,  $\rho_2 \approx 0.84701$ ,  $\rho_3 \approx 0.84701$ , and  $z_3 \approx (-3.0, 0.0)$ . Since the disks are not as well separated and the radii are larger than example (ii), this is the harder problem. Table 4 shows data for NFFT=256. We took NCGM=40 per Newton step. Notice that quadratic convergence is lost. In Fig. 5 we show an eigenvalue plot for the Newton step NN=4 corresponding to Table 4. The eigenvalues are clearly smeared out and CGM made considerably smaller progress. See Fig. 6 for graphics of the final map.

*Example (iv).* This is a 3 circle test, Fig. 7. In the previous examples our geometry had a lot of built in symmetry. The purpose of this example is to remove any type of symmetry and to take a mixture of different boundary curves. Boundary curve  $\Gamma_1$  is an ellipse with minor-to-major axis ratio  $\alpha_1 = 0.6$  - the middle object in Fig. 7. Boundary curve  $\Gamma_2$  is an inverted ellipse with  $\alpha_2 = 0.7$  - the top most object in Fig. 7. Boundary curve  $\Gamma_3$  is also an inverted ellipse with  $\alpha_3 = 0.5$  - the bottom most object in Fig. 7. Table 5 is the data for NFFT=256. We took initializations  $\rho_2 = 0.80$ ,  $\rho_1 = \rho_3 = 0.75$ ,  $z_3 = (0.1, -3.1)$ . Compare to final values  $\rho_1 \approx 0.808633$ ,  $\rho_2 \approx 0.872268$ ,

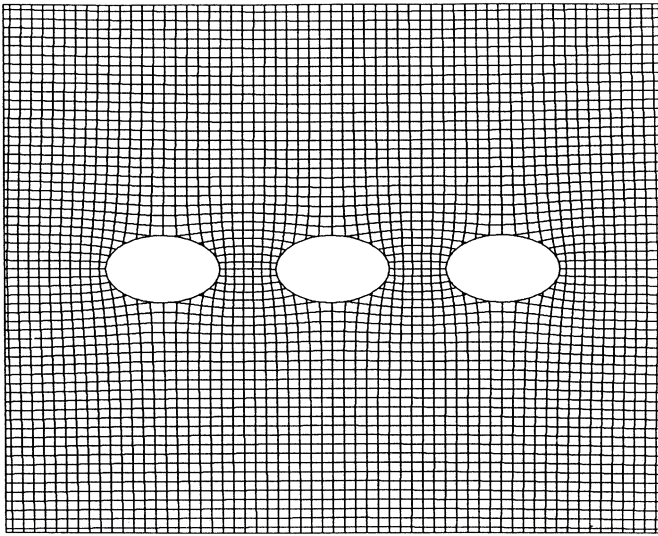


**Fig. 6.** Circle map for example (iii)

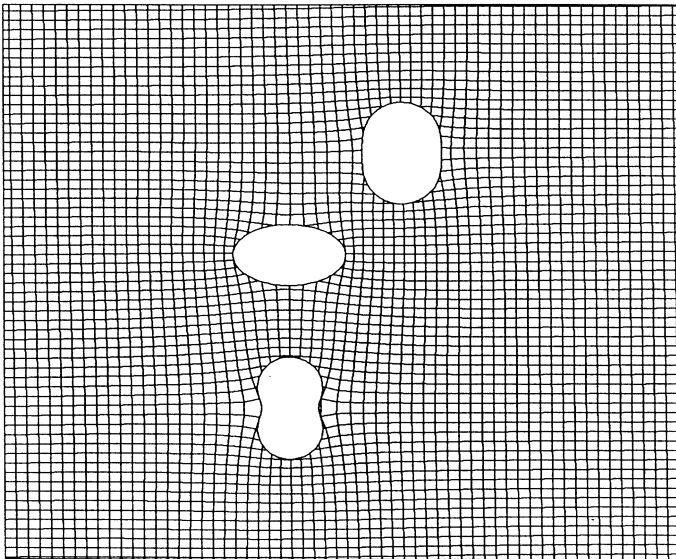


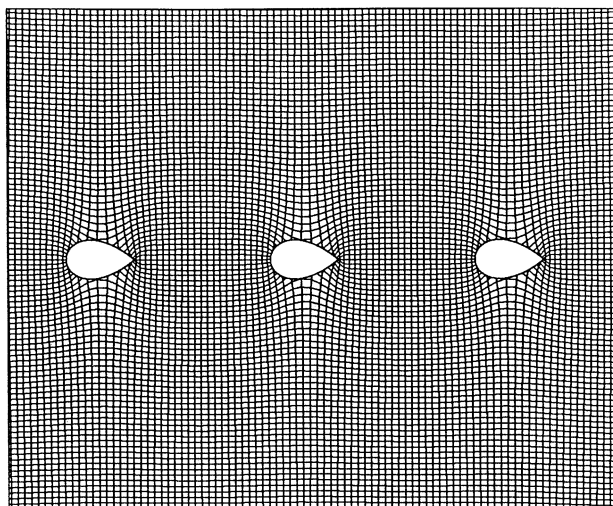
**Fig. 7.** Circle map for example (iv)

$\rho_3 \approx 0.8060864$ ,  $z_3 \approx (-0.005833, -2.98478)$ . As in example (iii) we expect this to be a difficult problem due to close circles and relatively large radii.

*Example (v). Multielement airfoil, Fig. 8.* The target boundaries are generated using lemniscates,  $a \cos b\theta$ , and meant to simulate airfoils. To use the

**Table 5.** Newton steps for example (iv). NFFT=256

NN	$ \delta\rho_1 $	$ \delta\rho_2 $	$ \delta\rho_3 $	$\ U_1\ _\infty$	$\ U_2\ _\infty$	$\ U_3\ _\infty$	$ \delta z_3 $
1	0.6e-01	0.7e-01	0.6e-01	0.1e-00	0.1e-00	0.2e-00	0.1e-00
2	0.3e-02	0.6e-02	0.1e-02	0.3e-01	0.4e-01	0.3e-00	0.4e-01
3	0.4e-03	0.4e-03	0.4e-04	0.4e-02	0.7e-02	0.2e-00	0.5e-02
4	0.3e-03	0.1e-03	0.1e-02	0.2e-02	0.3e-02	0.5e-01	0.4e-02
5	0.6e-05	0.4e-05	0.6e-04	0.2e-03	0.8e-03	0.1e-01	0.9e-04
6	0.2e-06	0.4e-06	0.7e-06	0.4e-04	0.2e-03	0.5e-03	0.1e-05
7	0.4e-07	0.1e-05	0.1e-05	0.3e-05	0.1e-04	0.6e-04	0.3e-05

**Fig. 8.** Circle map for example (v)

circle map, we first remove the corners of each blade by applying 3 successive Karman-Trefftz maps producing 3 nearly circular curves. The final map to the target airfoil domain is found by composing the circle map with the inverse Karman-Trefftz maps. The circle map has been used in the aircraft industry to compute flow around multielement airfoils [Ha]. More generally, a succession of explicit maps, such as the osculation maps of Grassmann described in [He], could be used to create nearly circular regions cheaply. The centers and average radii of the near-circles would then provide a good initial guess for our method.

*Example (vi). 3 Limacons, Fig. 9.* This example is self explanatory. We simply have a clustering of limacons. This example illustrates the conformal behavior of our circle map near the target boundaries. We take concentric circles and radial rays about each circle as the computational grid. This grid is not as global in nature as the xy orthogonal grid but in some sense it is more informative.

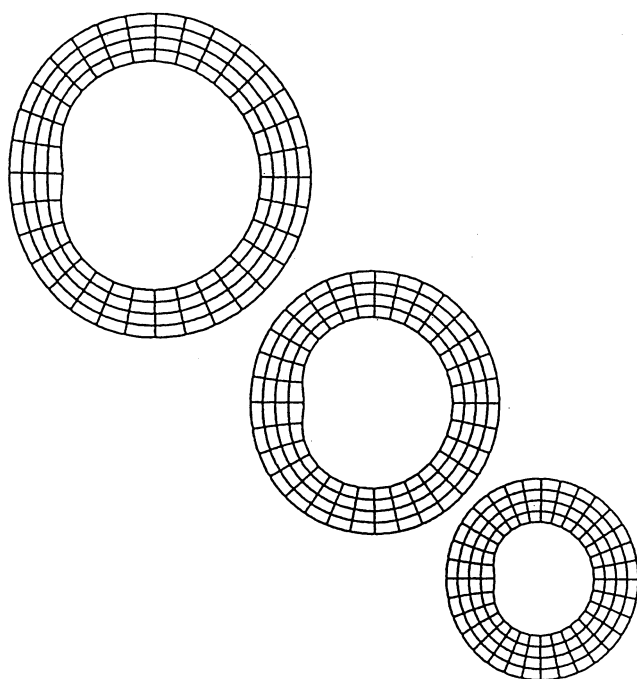


**Fig. 9.** Circle map for example (vi)

*Remarks.* (1) For regions of connectivity greater than 2, it is not always clear what the appropriate computational regions should be. The choice of a model or canonical domain may depend on both the problem one wishes to solve and the geometry of the target “physical” domain. Such questions, in fact, arise already for simply connected geometries, where, for instance, computing flow in a channel and resistances of elongated circuits, or handling the ill-conditioning of the mapping problem due to crowding for elongated regions require mapping from a rectangle or an ellipse; see the papers by DeLillo, Elcrat, and Pfaltzgraff [De, DE, DEP] for a discussion of these matters in the present context of Fourier series methods and for references to work of Driscoll, Gaier, Howell, Trefethen, Papamichael, Stylianopoulos, Wegmann and others on related questions for Schwarz-Christoffel and Riemann-Hilbert methods.

(2) The first algorithm developed to find the circle map is known as Koebe’s algorithm [He, notes at end of Chap. 17]. This algorithm was tested by Halsey in [Ha]. Koebe’s algorithm uses an iterative method which finds the normalized map from the exterior of some fixed boundary component to the exterior of the disk (thus perturbing the other components) and then alternates from component to component so that the computational domain becomes gradually more circular. The centers and radii of the circles are

found automatically in the process. A convergence proof for Koebe's algorithm due to Gaier can be found in [He]. The convergence is linear, but generally quite rapid. We are exploring more efficient formulations of our method to reduce the cost of the matrix-vector multiplications. Also, our matrices have a block structure determined by the connectivity which could be used to parallelize the matrix-vector multiplications. The Koebe algorithm apparently cannot be parallelized in this fashion.

General introductions to numerical conformal mapping are given in [Ga1] and [He]. A survey of the multiply connected case is given in [Ga2]. [Ell] computes the map to an annulus with circular slits using an expansion method and finding a minimax solution to a linear approximation problem. [KPS] use an orthonormalization method to compute the map to a disk or annulus with circular slits. Modifications of Symm's integral equation for single layer potentials are used by [Re] to compute the maps to an annulus with circular slits. [Ma] uses an integral equation formulation of Mikhlin to map to a disk with circular slits. [Am1, Am2, Am3] uses a method of fundamental solutions to map onto circular and radial slit domains. [Har1, Har2] uses a method involving matching potentials to map onto a region with arbitrarily specified boundary shapes such as rectangles with parallel sides. [Vol] uses a "block method" for the Laplace equation to map to regions with various geometries, including parallel slit and circular slit domains and infinite domains with periodic structure. An additional method which uses the circle geometry is given in [Pros].

## References

- [Am1] Amano, K. (1995a): Numerical conformal mapping onto the circular slit domains. *Trans. Inform. Process. Soc. Japan* **36**, 219–225 (in Japanese)
- [Am2] Amano, K. (1995b): Numerical conformal mapping onto the radial slit domains by the charge simulation method. *Trans. Japan SIAM* **5**, 267–280 (in Japanese)
- [Am3] Amano, K. (c. 1996): A charge simulation method for numerical conformal mapping onto circular and radial slit domains. *SIAM J. Sci. Comput.* **19** (1998), 1169–1187
- [De] DeLillo, T. K. (1994): The accuracy of numerical conformal mapping methods: a survey of examples and results. *SIAM J. Numer. Anal.*, **31**, 788–812
- [DE] DeLillo, T. K., Elcrat, A. R. (1993): A Fornberg-like conformal mapping method for slender regions. *J. Comput. Appl. Math.* **46**, 49–64
- [DEP] DeLillo, T. K., Elcrat, A. R., Pfaltzgraff, J. A. (1997): Numerical conformal mapping methods based on Faber series. *J. Comput. Appl. Math.* **83**, 205–236
- [DP] DeLillo, T. K., Pfaltzgraff, J. A. (1998): Numerical conformal mapping methods for simply and doubly connected regions. *SIAM J. Sci. Comput.* **19**, 155–171
- [Ell] Ellacott, S. W. (1979): On the approximate conformal mapping of multiply connected domains. *Numer. Math.* **33**, 437–446
- [Fo] Fornberg, B. (1980): A numerical method for conformal mappings. *SIAM J. Sci. Statist. Comput.* **1**, 386–400

- [Ga1] Gaier, D. (1964): *Konstruktive Methoden der konformen Abbildung*. Springer-Verlag, Berlin, Göttingen, Heidelberg
- [Ga2] Gaier, D. (1978): Konformen Abbildung mehrfach zusammenhängender Gebiete. *Jahresber. Dt. Math.-Ver.* **81**, 25–44
- [Go] Goluzin, G. M. (1969): *Geometric Theory of Functions of a Complex Variable*. Amer. Math. Soc., Rhode Island
- [Gr] Greenberg, M. D. (1998): *Advanced Engineering Mathematics*. Prentice-Hall, New Jersey
- [Ha] Halsey, N. D. (1979): Potential flow analysis of multielement airfoils using conformal mapping. *AIAA J.* **17**, 1281–1287
- [Har1] Harrington, A. N. (1982a): Conformal mappings onto domains with arbitrarily specified boundary shapes. *J. D'Anal. Math.* **41**, 39–53
- [Har2] Harrington, A. N. (1982b): Conformal mappings onto multiply connected regions with specified boundary shapes. In: *Numerical Grid Generation* (J. F. Thompson, Ed.), Elsevier, p. 601
- [He] Henrici, P. (1986): *Applied and Computational Complex Analysis, Vol. III*. John Wiley, New York
- [Ho] Horn, M. A. (1997): *Iterative Methods Applied to Some Problems in Conformal Mapping and Potential Theory*. PhD thesis, Wichita State Univ. Math. Dept., Wichita, KS
- [HK] Hoskins, W. D., King, P. R. (1972): Periodic cubic spline interpolation using parametric splines. *The Computer Journal* **15**, 282–283
- [KPS] Kokkinos, C. A., Papamichael, N., Sideridis, A. B. (1990): An orthogonalization method for the approximate conformal mapping of multiply-connected domains. *IMA J. Numer. Anal.* **9**, 343–359
- [LM] Luchini, P., Manzo, F. (1989): Flow around simply and multiply connected bodies: a new iterative scheme for conformal mapping. *AIAA J.* **27**, 345–351
- [Ma] Mayo, A. (1986): Rapid methods for the conformal mapping of multiply connected regions. In: *Numerical Conformal Mapping* (L. N. Trefethen, Ed.). Amsterdam: North-Holland, 125–142
- [Ne] Nehari, Z. (1952): *Conformal Mapping*. Dover, New York
- [Pros] Prosnak, W. (1977): Conformal representation of arbitrary multiconnected airfoil sections. *Bull. Acad. Polon. Sci., Ser. Sci. Techn.* **25**, 25–36 (591–602)
- [Re] Reichel, L. (1986): A fast method for solving certain integral equations of the first kind with application to conformal mapping. In: *Numerical Conformal Mapping* (L. N. Trefethen, Ed.). Amsterdam: North-Holland, 125–142
- [Vol] Volkov, E. A. (1994): *Block Method for Solving the Laplace Equation and for Constructing Conformal Mappings*. CRC Press, Boca Raton
- [Weg1] Wegmann, R. (1984): Convergence proofs and error estimates for an iterative method for conformal mapping. *Numer. Math.* **44** (1984), 435–461
- [Weg2] Wegmann, R. (1986a): On Fornberg's numerical method for conformal mapping. *SIAM J. Numer. Anal.* **23**, 1199–1213
- [Weg3] Wegmann, R. (1986b): An iterative method for the conformal mapping of doubly connected regions. *J. Comput. Appl. Math.* **14**, 79–98
- [Weg4] Wegmann, R. (1988): Discrete Riemann-Hilbert problems, interpolation of simply closed curves, and numerical conformal mapping. *J. Comput. Appl. Math.* **23**, 323–352
- [Weg5] Wegmann, R. (1996): Fast conformal mapping of an ellipse to a simply connected region. **72**, 101–126
- [Wid] Widlund, O. (c. 1981): On a numerical method for conformal mapping due to Fornberg. unpublished